The Coupling of a Two-Dimensional Hydrodynamic/Sediment Routing Model with an Upland Watershed Erosion Model in a Mountain Watershed, Red River, Idaho

Ahmed Bdour[1] and Thanos Papanicolaou [2]
1. Department of Civil Engineering, Hashemite University, Zarqa, Jordan
2. Iowa Institute of Hydraulic Research, the University of Iowa, Iowa City, USA

Abstract

In an effort to generate new knowledge and improved understanding of the complex interrelationships between watershed and instream parameters and the scale integrity influences on channel morphology, an integrated watershed hydrologic/sedimentation framework for mountainous watersheds is developed. This framework provides advanced analytical techniques and numerical models for simulating upland (macro level) and instream (micro level) processes in an integrated fashion. The framework is developed based on the premise that watershed-wide parameters have cumulative impacts on stream ecology and therefore, watershed modeling should facilitate integration of spatial and temporal scales in order to provide meaningful answers from the physical and statistical point of view. First, the GeoWEPP soil erosion model is employed to simulate the hydrologic, and sediment entrainment phenomena at the uplands of the Red River watershed, Idaho, USA. Long-term averages and different frequency distributions analyses are performed to investigate the temporal variability in upland soil erosion processes. Second, a thorough investigation for the particle transit time is performed using the hypsometric curve approach and the particle virtual velocity approach.

It is demonstrated that a fine sediment particle moves from the uplands to the mouth of the watershed within a relatively short period of time (few days). Third, this work also involves enhancing capabilities of an existing instream two-dimensional hydrodynamic/sediment transport model that was originally developed to simulate the transport of uniform sediments. The upland soil erosion model is eventually combined with the instream numerical model by matching the return period for a rainfall storm event for the upland soil erosion processes with instream flow that has the same return period for instream sediment transport processes. Finally, modeling results are compared with 13-year detailed field data and against the predictions of commercial and private

models, including the USACE models (RMA2 and SED2D) and the 3ST1D model developed in-house.

Keywords: Watershed Modeling, Scale Integration, Soil Erosion, Sediment Transport, Particle Transient Time

Introduction

Issues related to the decline of salmon and other fish populations in the Pacific Northwest are reaching national priority status through the Clean Water Act and the Endangered Species Act (Hatfield and Bruce, 2000; Slaughter *et al.*, 2000). Many efforts to restore aquatic and riparian habitat have failed because their designs did not account for the complex interrelationships between the affecting parameters within a watershed and scale integrity influences on channel morphology. The interdisciplinary nature and increasing complexity of environmental and water-resource problems require the use of modeling approaches that can incorporate knowledge from a broad range of scientific disciplines. The selection of an individual (e.g., ecology, watershed hydrology, sediment transport) model to address watershed processes is not feasible, given the large number of processes, their dynamics and interactions, and the scales that these processes occur on. Coupled with these issues are the problems of study area characterization and parameterization (Jagger *et al.*, 1997). Guidelines for parameter estimation are sparse, and the user commonly has to make decisions based on an incomplete understanding of the relation between parameter values and physical measures of watershed characteristics.

Research methodology

In building this integrated framework to apply to the case study, and then considering its implications, some directions have been developed that are either new, or are taken beyond the point previously reported in the literature. In order to successfully complete this integration, spatial and temporal scales variability of watershed dynamic features are thoroughly investigated in the course of this research. These directions are introduced below and their development is further reported in subsequent sections.

Spatial and Temporal Scale Variability

The backbone of the spatial and temporal scale approach is well depicted in Figure 5, where the *x-axis* denotes time and the *y-axis* denotes space. Figure 5 shows that there are three distinct spatial scales were considered in our integrated approach: namely, (1) local/habitat scale; (≈10m), instream flow and sediment transport, and channel response are simulated using an enhanced 2-D instream hydrodynamics and sediment transport model coupled with soil erosion model, including the impacts of land management practices, sediment travel distance, and mean residence time, (2) sub-regional/reach scale (≈100m), a process-based upland soil erosion model is used for evaluating rainfall/runoff volumes, sediment yield frequency analysis, and long-term upland soil erosion predictions, and (3) regional/ watershed scale (≈10^3m) analysis consists of the entire river basin watershed and its associated channels. At this scale, simulations include sediment and water routing, sediment travel time, and channel response through the entire sediment region. The composite tool provides the capability to conduct both broad regional-level and sub-regional/local level detailed studies with feedback mechanisms.

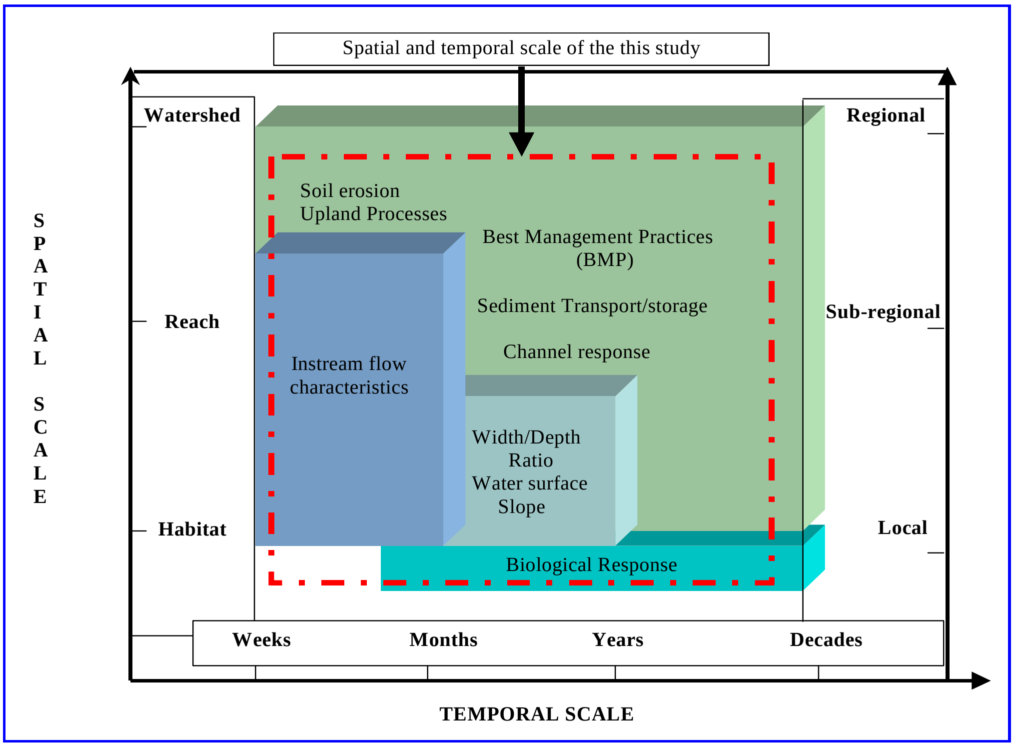

Figure 1: Spatial and Temporal Scale Features of this Study.

The integration processes modeled in this study for the Red River watershed are limited to time scales described in years and not in decades. It is not expected, therefore, the integration model to pinpoint significant geomorphologic changes due to the channel response to sediment influx from the uplands and flow action.

Particle Transit Time Approaches

Sediment particles move from slopes to 1st order streams and through stream networks (1st order and 2nd order streams) by a variety of processes (i.e., weathering, landslides, catastrophic or storm events). Defining particle transit distance and time is of great importance in watershed processes modeling. This issue has not been adequately resolved, particularly with respect to the fine particles (silts and clays), which are often the most problematic (Bonniwell *et al.*, 1999). Researchers do not know the time-lag between soil erosion process and instream transport (how quickly sediment will propagate downstream and how fast it will spread). Therefore, magnitude, timing, and duration of downstream changes in sediment transport cannot be predicted effectively.

The presented work is a first attempt to bridge the gap in our knowledge and addresses the aforementioned concerns. The particle transit time is investigated in this study at three levels based on the correct understanding of the gross paths taken by sediment particles in a watershed. *Path-1* is defined as the travel time for sediment to move from its original location to stream networks (tributaries). *Path-2,* sediment particles travel from the stream networks to the mainstem. *Path-3* occurs when sediment travels through the mainstem and ends up at the mouth of the watershed (Figure 2). The most recent studies cited in the literature are employed for determining the particle transit time and distance for each path. For *path-1*, the concepts of the hypsometric curve analysis approach (Luo and Harlin, 2003) and the particle virtual velocity (Papanicolaou and Knapp, 2002) are applied. For *path-2 and path-3,* the findings of radionuclides tracing studies (Bonniwell *et al.*, 1999; McGlynn *et al.*, 2003) are adopted. Description of each of these methods is presented below.

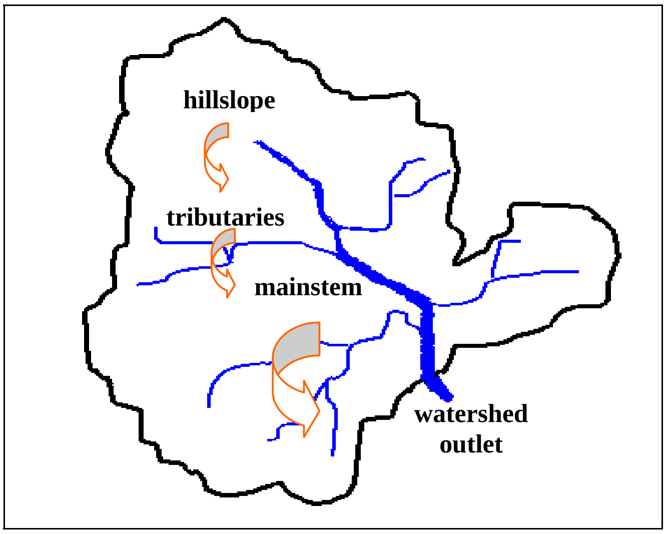

Figure 2: Schematic Representation For Sediment Travel Paths Within A Watershed.

(a) Hypsometric Curve Approach (Path-1)

This approach will help in determining the minimum travel time of a raindrop and set a travel time threshold. The advantage of this approach is that it takes the overall basin slope, rather than the local slope, into consideration and it is directly linked to the potential energy distribution throughout the basin.

Luo and Harlin (2003) considered a simple approach to determine the travel time of a water drop moving down an impermeable and frictionless surface characterized by the basin's hypsometric curve. The hypsometric curve is derived from watershed topography and is assumed to be represented by a third degree polynomial function of the form ($y=c_o+c_1x+c_2x^2+c_3x^3$). Luo and Harlin assumed this travel time depends only on the tangential component of gravity and associated acceleration and the overall slope of the watershed (represented by its hypsometric curve, Figure 3). Figure 4 illustrates the force analysis considered in the hypsometric approach.

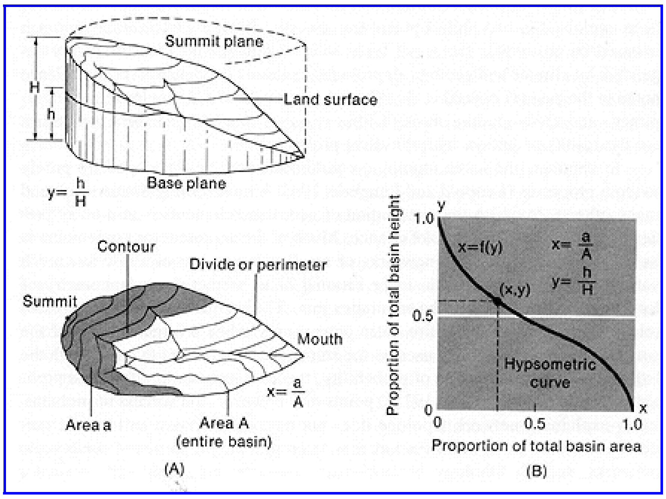

Figure 3: Schematic Diagram Illustrating The Hypsometric Curve and The Variables Involved (*a*=area of the basin above height *h*; h= height above outlet; *A*= total area of basin; and *H*= total relief of the basin). (Source: Strahler, 1952)

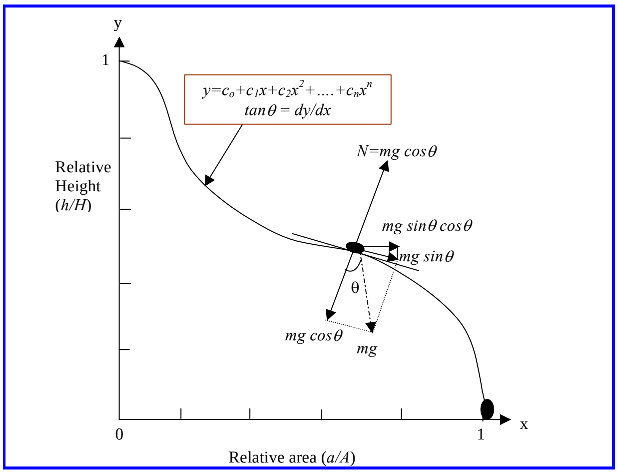

Figure 4: The Force analysis of A Water Drop Moving Down Frictionless Surface Represented By The Hypsometric Curve of A Watershed Basin (*g*= gravitational acceleration constant; a= acceleration in the direction parallel to the tangent of the slope at *x*=*x; m*= mass of the drop of water; and θ = slope angle at *x*=*x* where *tan* θ =*dy/dx*). (Source: Luo and Harlin, 2003)

The Luo and Harlin (2003) theoretical travel time expression is:

$$t = \sum_{x=\Delta x/2}^{l} \frac{\Delta x}{\sqrt{2\sum_{x=\Delta x/2}^{x}(a_x \Delta x)}} = \sum_{x=\Delta x/2}^{l} \frac{\Delta x}{\sqrt{2\sum_{x=\Delta x/2}^{x}\left(g\frac{c_1+2c_2x+3c_3x^3}{1+(c_1+2c_2x+3c_3x^2)^2}\Delta x\right)}} \qquad (1)$$

(b) Virtual Velocity Concept (Path-1)

The virtual velocity concept is a physically-based concept. Expressions for the particle virtual velocity are developed based on the Buckingham π theorem and image analysis laboratory data for tracking particle displacement. The form of the derived equations are expressed as

$$u_{sv} = \sqrt{\frac{\rho_s-\rho}{\rho}gd}\left[0.073\frac{du_*}{k_s\omega}\sqrt{1-\frac{\left(\frac{u_{*c}}{\omega}\right)}{\left(\frac{u_*}{\omega}\right)}}\right] \quad \text{for} \quad 0 \le \left(\frac{d}{k_s}\right)\left(\frac{u_*}{\omega}\right)\sqrt{1-\frac{\left(\frac{u_{*c}}{\omega}\right)}{\left(\frac{u_*}{\omega}\right)}} \le 0.14 \qquad (2a)$$

$$u_{sv} = \sqrt{\frac{\rho_s-\rho}{\rho}gd}\left[3.25\frac{du_*}{k_s\omega}\sqrt{1-\frac{\left(\frac{u_{*c}}{\omega}\right)}{\left(\frac{u_*}{\omega}\right)}}-0.45\right] \quad \text{for} \quad 0.14 < \left(\frac{d}{k_s}\right)\left(\frac{u_*}{\omega}\right)\sqrt{1-\frac{\left(\frac{u_{*c}}{\omega}\right)}{\left(\frac{u_*}{\omega}\right)}} \le 0.2 \qquad (2b)$$

$$u_{sv} = \sqrt{\frac{\rho_s-\rho}{\rho}gd}\left[1.7\frac{d\ u_*}{k_s\,\omega}\sqrt{1-\frac{\left(\frac{u_{*c}}{\omega}\right)}{\left(\frac{u_*}{\omega}\right)}}+0.10\right] \quad \text{for} \quad \left(\frac{d}{k_s}\right)\left(\frac{u_*}{\omega}\right)\sqrt{1-\frac{\left(\frac{u_{*c}}{\omega}\right)}{\left(\frac{u_*}{\omega}\right)}} > 0.2 \qquad (2c)$$

where u_{sv} is particle virtual velocity; ρ_s, ρ are the density of sediment and water, respectively; u_* is the friction velocity; u_{*c} is the critical friction velocity; d is the diameter of the entrained material; and k_s is the roughness of the bed material.

Results and Discussion

Upland Modeling Results

The soil erosion modeling work presented in this paper falls into two parts. First, information is presented on approaches to automatically delineate watersheds into hillslopes and conduct WEPP model simulations. Second, sediment yield predictions are introduced based on both long-term averages and frequency distribution for rainfall storm events.

For all subwatersheds, the FENN RS ID climate station was chosen automatically by the model, which is located closest to the watershed outlet. Forest silt loam soil type was assumed for this watershed (Elliot and Miller, 2002; N. Gerhardt, pers. comm., 06/2002). The other model input parameters are shown in Table 1. All model runs were conducted for 50 years as recommended by (Baffaut *et al.*, 1996).

Table 1: Summary of The GeoWEPP Input Data and Sediment Yield Predictions for the Entire Main Fork Red River Watershed.

Sub#	Area (ha)	Sed. Load (ton/yr)	Sed. yield (tons/ha/yr)	CSA (ha)	Simulation time (yrs)	MSCL (m)	WEPP soil	WEPP land use
1a	257.25	10.1	0.04	30	50	100	20-yr forest silt loam	85% cover
1b	473.94	31.9	0.07	30	50	100	20-yr forest silt loam	85% cover
1c	738.32	42.5	0.06	30	50	100	20-yr forest silt loam	85% cover
2	1158.1	58.2	0.05	30	50	100	20-yr forest silt loam	88% cover
3	1792.9	413.1	0.23	30	50	100	20-yr forest silt loam	84% cover
4	979.82	115.5	0.12	30	50	100	20-yr forest silt loam	Forest (100% cover)
5	930.52	566.4	0.61	30	50	100	20-yr forest silt loam	94% cover
6	1284.4	806.4	0.63	30	50	100	20-yr forest silt loam	94% cover
7	124.7	4.3	0.03	30	50	100	20-yr forest silt loam	94% cover
8	358.72	33.2	0.09	30	50	100	20-yr forest silt loam	94% cover
9	1313.71	194.9	0.15	30	50	100	20-yr forest silt loam	80% cover

Long-term Averages

The modeling runs were carried out for the nine subwatersheds. The results were converted into units of tons/ha/yr and introduced in both numeric and map presentations in Table 1 and Figure 5, respectively, for all subwatersheds.

The summary in Table 1 shows that Main Fork Red River watershed generates a total sediment load of 2276.5 tons/yr and this load produces average annual sediment yield of 45.8 tons/mi^2. The annual sediment yield rate for individual subwatershed varies from 0.03 to 0.63 tons/ha/yr, for subwatershed (7) and subwatershed (6), respectively. It is important to note that the high elevation subwaterhseds (uplands), namely, subwatersheds (4), (5), (6) and (7) generate 65% of the total generated sediments. Instead, lowland subwatersheds, namely, subwatersheds (1a, 1b, 1c, and 2) generate only 6%, and the remaining 29% generated by moderate elevation subwatersheds (subwatersheds (3, 4, 7, 8, 9)).

We compared the predicted soil erosion rates with the values predicted by Gloss (1995) using NEZSED model for the same study area (Harmon *et al.*, 1992). Table 2 shows a summary of this comparison. The results indicate that the GeoWEPP model overestimates the observed sediment yields with a magnitude of 1 ½. NEZSED model predicts only about 1/3 of observed sediment yield.

Table 2: Sediment Yields Comparison with Gloss Study (1995).

Prediction method	Average annual sediment yields (tons/mi^2)	Error %
Predicted using GeoWEPP model	45.80	51.0
Predicted using NEZSED mode	11.73	61.3
Observed (1986-1993)	30.33	0.0

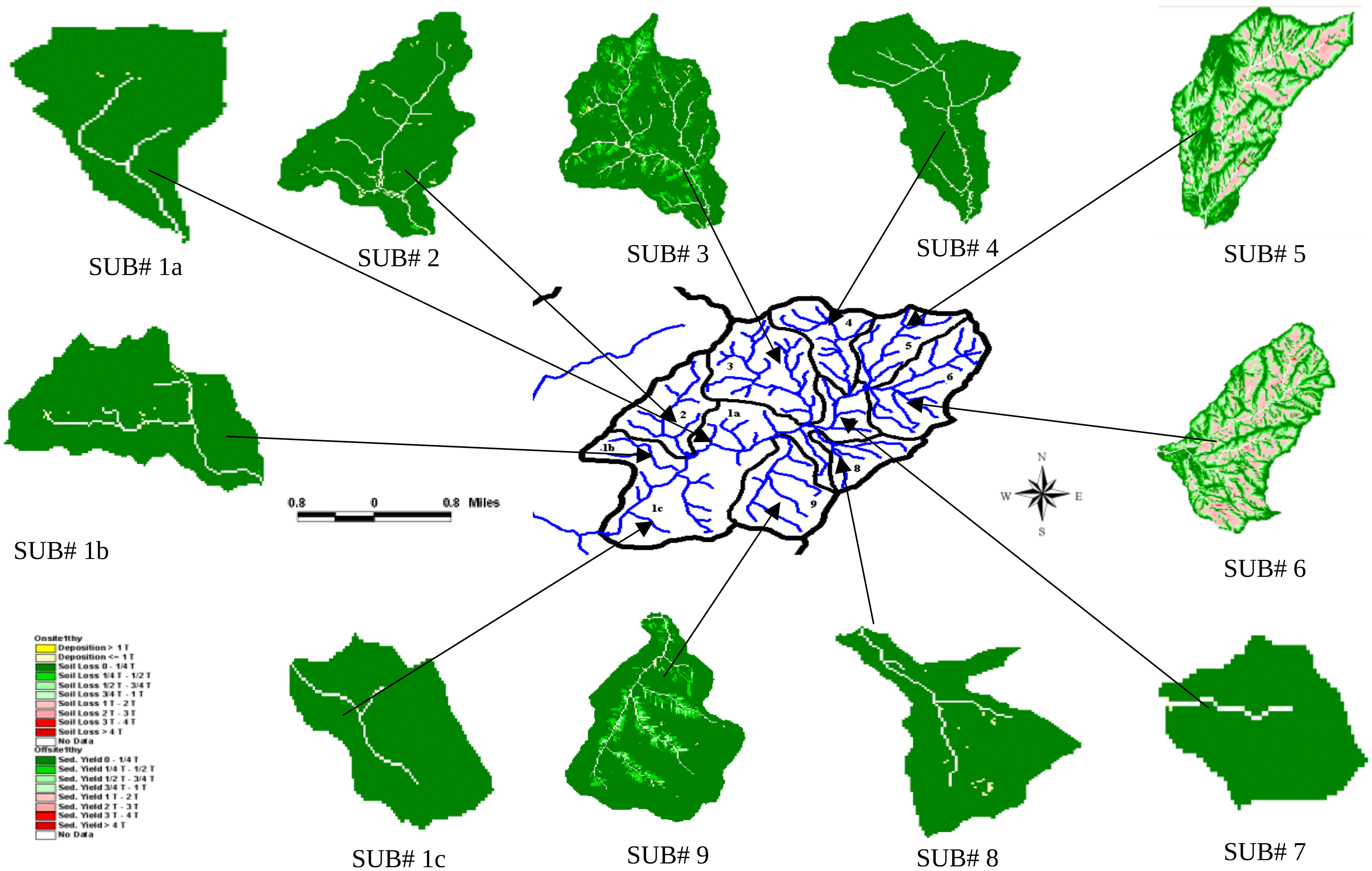

Figure 5: Soil Erosion Modeling Results for the Entire Main Fork Red River Watershed.

Frequency Distribution Analysis

The GeoWEPP long-term averages for sediment yield predictions are higher by 1 ½ orders of magnitude and do not account for the temporal variability in climate or the dynamics in soil erosion processes. More importantly, in an integrated modeling framework it is inaccurate to simulate processes without connecting the temporal and spatial scales. A more suitable measure of soil erosion rates is a probabilistic approach using a frequency distribution analysis, which considers both the scale variability and addresses the dilemma of coupling.

For this purpose, we utilize the capabilities of the WEPP model in the watershed mode to perform a frequency distribution analysis for storm events. The model is run for the nine subwatersheds within the Main Fork Red River watershed. The weather climate generator, CLIGEN, is used to generate a 100-year climate file. The storms of 2-, 5-, 10-, and 25-year return periods are selected for the purpose of this analysis. The same procedures were applied to all subwatersheds of the Main Fork Red River.

Figure 6 demonstrates the frequency distribution of the sediment yields for the four rainfall storm events. Results show that only three subwatersheds within the entire Main Fork Red River were contributors in sediment production, specifically, subwatershed (1a), subwatershed (8), and subwaterhsed (1b), generated sediment yields of 5.6 tons/day, 4.9 tons/day, and 0.1 tons/day, respectively, with a 2-yr return period storm event. The remaining subwaterheds have zero sediment delivery rates.

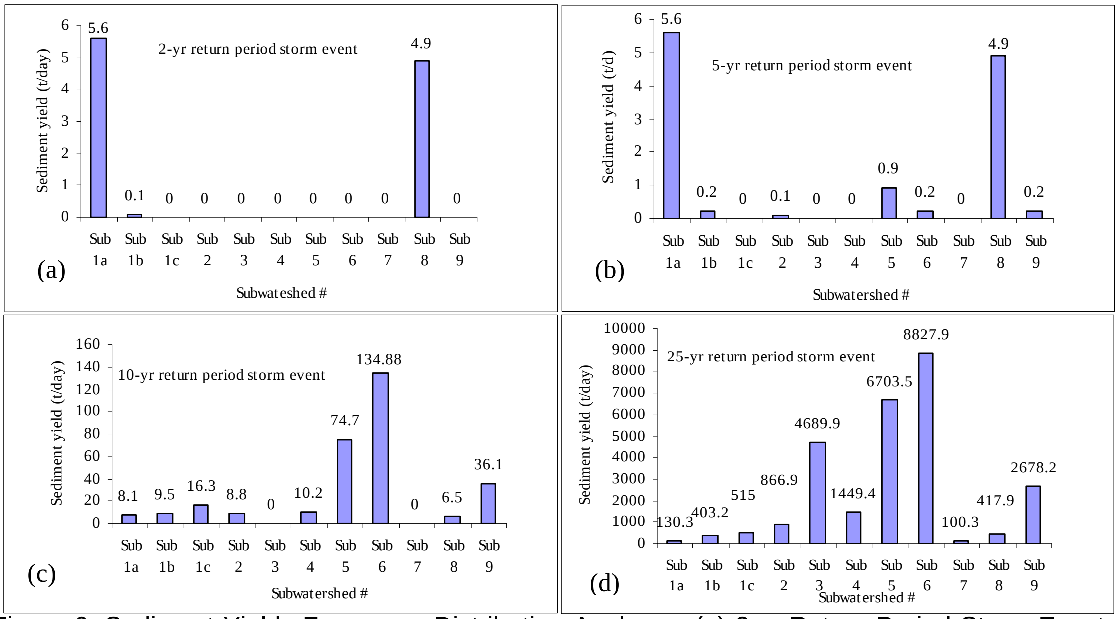

Figure 6: Sediment Yields Frequency Distribution Analyses, (a) 2-yr Return Period Storm Event, (b) 5-yr Return Period Storm Event, (c) 10-yr Return Period Storm Event, and (d) 25-yr Return Period Storm Event.

In order to justify these results, Table 3 is introduced. It presents the topographic characteristics for each subwatershed, including the rainfall volumes and average water depths for the 2-yr storm event. Subwaterhseds (1a) and (8), which generated most of the sediments have smaller drainage areas, higher precipitation depths (for this particular storm), and higher gradients as compared to the remaining subwatersheds. This justifies the predicted sediment yield rates for these subwatersheds.

Table 3: Subwatershed Characteristics, Rainfall Volumes, Average Flow Depths and Gradients for 2-yr Storm Event.

Col. 1	Col. 2	Col. 3	Col. 4	Col. 5
Sub#	Area (ha)	Volume Runoff (m^3)	Avg. water depth (m)	Avg slope
Sub 1a	257.25	7495.50	0.00291	0.32
Sub 1b	473.94	2817.00	0.00059	0.14
Sub 1c	738.32	4349.00	0.00059	0.20
Sub 2	1158.10	6669.00	0.00058	0.22
Sub 3	1792.9	11565.00	0.00065	0.15
Sub 4	979.82	5894.00	0.00060	0.24
Sub 5	930.52	10634.00	0.00114	0.17
Sub 6	1284.4	14000.00	0.00109	0.20
Sub 7	124.70	759.00	0.00061	0.21
Sub 8	358.72	9584.00	0.00267	0.29
Sub 9	1313.71	7635.00	0.00058	0.19

We compared the predicted sediment delivery rates for the 2-yr storm event and for the 10-yr storm event with the measured suspended loads in the Red River watershed (Figure 7). The WEPP model predicts a total of 10.6 tons/day and 305.08 tons/day for the two storm events, respectively. Comparison shows that the 2-yr WEPP prediction is in good agreement with the measured suspended load at the bankfull discharge (instream flow of 9.4 m^3/sec), which is 14.46 tons/day. On the contrary, the 10-yr WEPP prediction is 305 tons/day, which is almost twenty times the magnitude of the measured value.

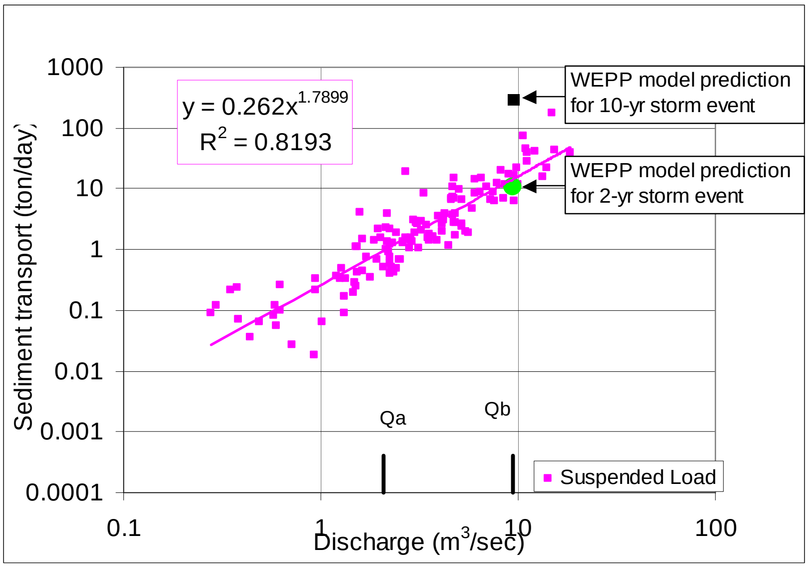

Figure 7: Measured Suspended Load in the Main Fork Red River and WEPP Predictions for the 2-yr and 10-yr Storm Event.

In the current work, coupling the soil erosion model with the instream sediment transport model is accomplished by matching the 2-yr climatic model WEPP prediction for soil erosion rate with the magnitude of 2-yr instream flow. The 2-yr storm event sediment delivery rate (10.6 tons/day) is then used as a sediment influx boundary condition in the instream modeling component with the bankfull discharge as the instream modeled flow, to investigate channel geomorphology and sediment transport. Instream model input data and boundary conditions will be discussed later in coarse of this research.

The matching assumption is only valid if there is no lag time between the upland soil erosion process and the instream sediment transport process (main channel), sediment particles move from the uplands to tributaries (*Path-1)* and then enter the main channel (*Path-2*) in a relatively short period of time. To determine particle travel time, the best available concepts cited in the literature were used, including the GIS based method that is called the hypsometric curve approach (Luo and Harlin, 2003) and the particle virtual velocity approach (Knapp, 2002; Papanicolaou and Knapp, 2002).

Particle Transit Time Results

As discussed earlier in this paper, the particle transit time from the uplands to the stream network (*Path-1)* has been determined using the hypsometric curve analysis approach (Luo and Harlin, 2003) and the concepts of particle virtual velocity (Knapp, 2002; Papanicolaou and Knapp, 2002) and. The next sections briefly introduce the methodology and calculation procedures for each approach

.

(a) Hypsometric Curve Calculations

The hypsometric curves of the nine subwatersheds (the entire Red River watershed) and the polynomial fits are obtained using an automated Geographic

Information System (GIS) and the input data comes from a 7.5 minute Digital Elevation Model (DEM), downloaded from the US Geological Survey (USGS); see (Luo, 1998) for detailed procedures. Then, the *x-axis* (relative area) is normalized by dividing the area above different elevations (*a*) by the total area (*A*) above the exit of the subwatershed (Figure 8). Similarly, for the *y-axis* (relative height), the elevation is normalized by dividing the elevation of each contour (*h*) by the total elevation/relief (*H*). The GIS is used to calculate the areas of the polygons formed by adjacent contour lines and the subwatershed boundary. Data points for each subwatershed *(a/A) vs. (h/H)* are plotted (Figure 8) and the best-fit 3rd degree polynomial functions are obtained (Table 4).

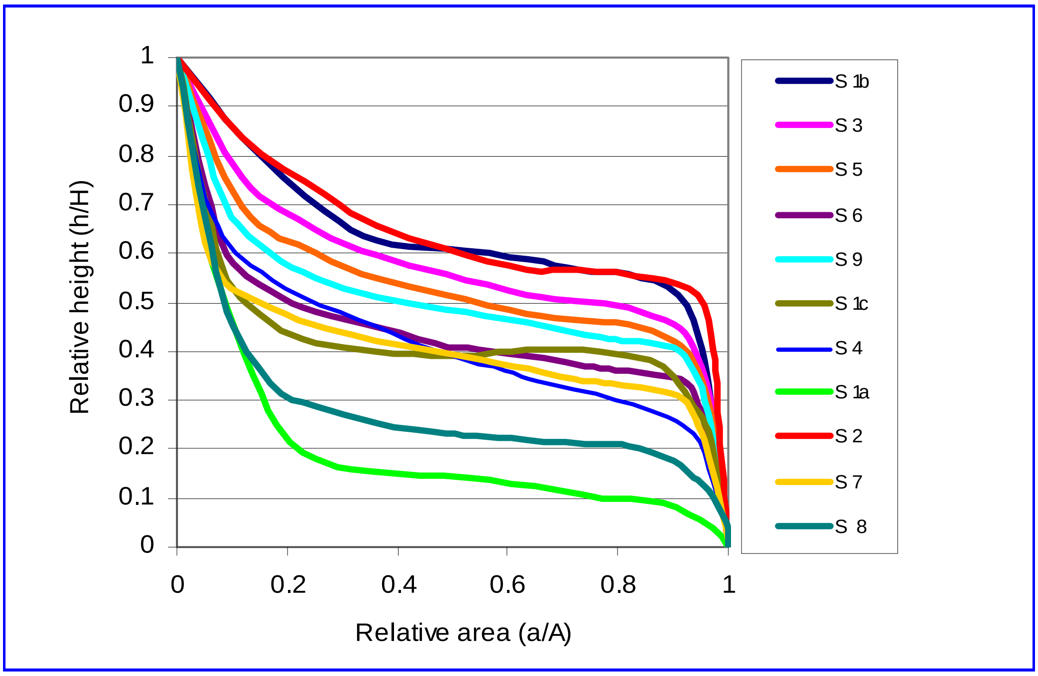

Figure 8. Hypsometric Curves of the Nine Subwatersheds Within the Main Fork Red River Watershed.

Table 4: Polynomial Functions for Hypsometric Curves of the Nine Subwatersheds Within the Main Fork Red River Watershed.

Subwatershed #	Polynomial function form*
Sub 1a	$Y = -4.398X^3 + 6.3804X^2 - 2.893X + 1.0448$
Sub 1b	$Y = -4.4867X^3 + 8.14958X^2 - 4.5966X + 0.904$
Sub 1c	$Y = -4.611X^3 + 7.9258X^2 - 4.2083X + 0.9101$
Sub 2	$Y = -4.4618X^3 + 7.1354X^2 - 3.5449X + 0.9525$
Sub 3	$Y = -3.6006X^3 + 5.9347X^2 - 3.2188X + 0.9445$
Sub 4	$Y = -4.4739X^3 + 6.9189X^2 - 3.3352X + 0.9885$
Sub 5	$Y = -4.2561X^3 + 6.5047X^2 - 3.1472X + 1.007$
Sub 6	$Y = -4.1564X^3 + 6.2026X^2 - 2.9453X + 1.0207$
Sub 7	$Y = -4.117X^3 + 6.6011X^2 - 3.3222X + 0.9048$
Sub 8	$Y = -3.8057X^3 + 5.5617X^2 - 2.6093X + 1.04$
Sub 9	$Y = -5.5093X^3 + 8.7418X^2 - 4.1112X + 0.9463$

* Y: relative height (h/H) and X: relative area (a/A)

(b) Virtual Velocity Calculations

The distributions of primary particles in the eroded sediments are obtained from the output of the WEPP model for the each subwatershed to determine the entrained particle diameter (*d*) and the surface roughness, k_s, in Equation (2). These values are shown in Table 5. The Dietrich (1982) formula is used to calculate the particle falling velocity, ω, for nonspherical particles, as follows,

$$\log \omega_* = -3.76715 + 1.92944(\log D_g) - 0.09815(\log D_g)^2 - 0.00575(\log D_g)^3 + 0.00056(\log D_g)^4 \qquad (3)$$

where ω_* is the dimensionless falling velocity; and D_g is the dimensionless grain diameter, expressed as

$$D_g = \frac{(\rho s - \rho) g d^3}{\rho v^2} \qquad (4)$$

where *d* is the diameter of the entrained material, and

$$\omega = \left(\frac{(\rho s - \rho) g v \omega_*}{\rho} \right)^{1/3} \qquad (5)$$

The friction velocity, u_*, and critical friction velocity, u_{*_c}, are calculated following Papanicolaou *et al.* (1999) study. Values for the average water depths are obtained by dividing the runoff volume by the subwatershed area. Average slopes and length for each subwatershed are obtained from the WEPP model, the watershed mode. The length considered in the calculations is the longest distance between the subwatershed boundary and tributaries. Table 5 summarizes the calculated input parameters for Equation (2) and the computed particle virtual velocities and travel times. Results show that using the hypsometric curve approach the particle may take only 40-296 seconds to move from the uplands to the stream network (column 9). However, using the virtual velocity approach a sediment particle may take 0.87-14.36 days to move the same distance (column 8). As expected, the hypsometric curve approach introduces a minimum travel time threshold (considering impermeable and frictionless surface), while the particle virtual velocity approach provides reasonable range for the travel times. This may be justified based on the fact that virtual velocity equations are derived from dimensional analysis, which considers most of the significant parameters (i.e., flow depth, gradient, surface roughness, entrained sediment diameter, friction velocity, etc). Furthermore, the equations used were calibrated and corrected using experimental data on the motion of individual particle (Knapp, 2002).

Table 5: Input Parameters For Virtual Velocity Equations and Computed Particle Travel Times Using Both Methods

Col. 1	Col 2	Col. 3	Col. 4	Col. 5	Col. 6	Col. 7	Col. 8	Col. 9
Sub#	*Length (m)*	d_s *(mm)*	k_s *(3*d_{90}*) (mm)*	ω_* *(eq. 3) dimensionless*	ω *(eq. 5) (m/sec)*	u_{sv}*(eq. 2c) (m/sec)*	*Travel time* (day)*	*Travel time** (sec)*
Sub 1a	641.97	0.055	2.04	0.00068	0.00233	0.00858	0.87	39.88
Sub 1b	1158.51	0.064	2.55	0.00158	0.00308	0.00247	5.43	81.67
Sub 1c	1641.98	0.059	2.43	0.00101	0.00265	0.00291	6.53	166.66
Sub 2	2533.65	0.072	2.58	0.00300	0.00381	0.00301	9.75	276.17
Sub 3	4129.87	0.085	2.16	0.00722	0.00511	0.00333	14.36	313.87
Sub 4	2473.22	0.068	1.77	0.00220	0.00344	0.00431	6.65	295.55
Sub 5	2440.86	0.081	2.01	0.00561	0.00469	0.00464	6.08	206.25
Sub 6	2867.41	0.076	2.82	0.00400	0.00419	0.00356	9.33	279.57
Sub 7	277.88	0.084	2.94	0.00679	0.00500	0.00292	1.10	101.32
Sub 8	887.20	0.088	2.22	0.00866	0.00542	0.00816	1.26	76.35
Sub 9	2854.20	0.079	2.07	0.00491	0.00449	0.00349	9.46	265.44
Trail Creek	9187.39	0.085	2.16	0.00722	0.005107	0.1825	0.583	NA
Bridge Creek	6596.90	0.081	2.01	0.005608	0.004694	0.1373	0.556	NA

*Travel time calculated using the particle virtual velocity approach
**Travel time calculated using the hypsometric curve approach

In conclusion, the travel time calculations demonstrate that a fine sediment particle moves from the uplands to the network of the Red River watershed within a relatively short period of time (few days). Therefore, the assumption that there is approximately no significant lag time between the sediment generated at the uplands and that which transported in the stream is valid.

Instream Sediment Transport Modeling Results

After calculating the sediment influx from the uplands using the GeoWEPP model, EnSEDZL model is used to simulate the resuspension, deposition, and multifractional bedload transport of sediments and the resulting changes in the bathymetry in the lower part of the Main Fork Red River. The purpose of this work is to test our coupling hypothesis of matching the return period for a rainfall storm event for the upland soil erosion processes with instream flow that has the same return period for instream sediment transport processes. Therefore, two different modeling scenarios are designed; (1) the matching scenario, in which the 2-yr storm event for sediment yield predictions were used as a boundary condition; and (2) the mismatching scenario, in which the 10-yr storm event for sediment yield predictions are used. The instream modeling flow in both scenarios was the bankfull discharge (~2-yr return period flow event). For verification of the model, results of numerical calculations of changes in bed bathymetry due to erosion and deposition are compared with the bathymetric measurements taken at two transects of the river in 1995 and 1998. Results for bedload sediment transport rates are compared with field measurements for flow and fractional sediment taken between water years 1986 to 1999. Also, the results are compared with the other models prediction, namely, 2-D depth-averaged hydrodynamic model (RMA2, King and Orlob, 1973), 2-D single size class sediment transport model (SED2D-WESv1.2, Roig, *et. al.,* 1996), and Steep Stream Sediment Transport model (3ST1D), Papanicolaou *et al.*, 2004). A detailed description of the model input, modeling calculations, and verification is presented in the following section.

Model Input Data

Extensive set of data were obtained from the Nez-Perce National Forest Service, Idaho, on the flow rates, suspended and bedload sediment transport rates, sediment sizes, channel geometry, longitudinal profiles for stream bed elevation and water surface elevations. The data pertinent to the present modeling work are briefly reviewed in the following sections.

Figure 9 shows the depth-averaged velocity contours in the reach (in *m/sec*). The velocities are the greatest in the narrower parts of the channel and in the middle of the channel, and they decrease significantly in the wider parts of the channel.

Figure 10 shows the simulated contours for the bed shear stress in the modeled reach. The bed shear stress distribution follows the same trend as velocity contours in Figure 10, with the bed shear being higher in the narrower parts, values range from 21 to 45 N/m^2, and decreasing when the channel width increases with a range between 3 to 15 N/m^2. Basically, the patterns of the bed shear stress and velocity are affected by channel plan geometry in addition to the bed topography. Most notably, the channel width constricts to roughly 10 m at the middle. It is this constriction that results in the occurrence of the standing peak zone of bed shear stress and velocity in this part of the channel. Channel constriction is known to lead to increased bed shear stress and subsequently, to local scour of the bed (Lim, 1993; Lim and Cheng, 1998).

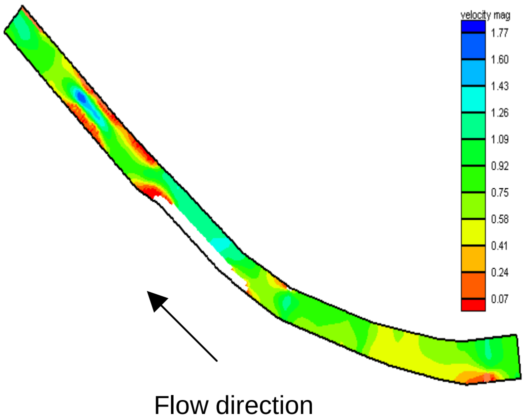

Figure 9: Calculated Flow Velocity Contours in the Modeled Reach.

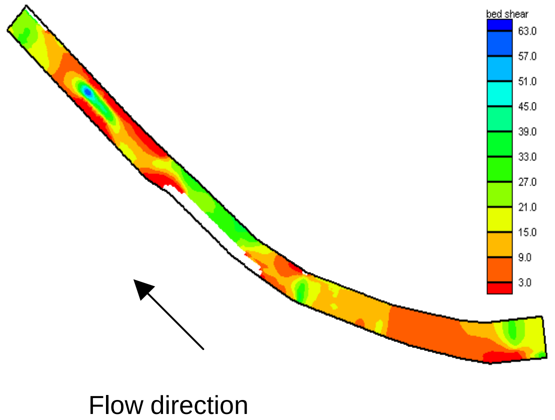

Figure 10: Bed Shear Stress Distribution in the Modeled Reach
(in N/m^2).

Sediment Transport Modeling:

The sediment transport modeling setup in this study was designed to meet the following objectives:

- To test the coupling hypothesis of the soil erosion model with the instream transport model by matching the recurrence interval of the instream flow and the rainfall event for soil erosion;
- To verify soil yield predictions by analyzing the long-term effects of river-development on channel morphology and the channel response to the increase in sediment influx; and
- To compare EnSEDZL model capabilities with other 2-D and 1-D hydrodynamic and sediment transport models and to emphasize on the limitations of each model for engineering modeling applications.

In order to meet the aforementioned objectives, we ran the model for two different scenarios. In the first scenario, it was assumed that the upstream suspended sediment load input is the GeoWEPP sediment yield predictions with a 2-yr recurrence rainfall storm event. While in the second scenario suspended sediment input at the upstream boundary was assumed to be the predictions for a 10-yr recurrence interval. The results of the sediment transport modeling are presented in great detail in the following sections.

Figure 11 shows the modeling calculations for the first scenario. A negative sign indicates scour and a positive sign indicates deposition. Results show that the streambed for this case was exposed to sequences of erosion and deposition processes. The erosion/scour depths range from 2 to 12 cm. The peak zones of erosion took place in the narrowest parts of the channel.

Appreciable erosion spots were noticed also at the entrance of the channel, at the channel bend, and towards the end of the channel. Bed deformations patterns are consistent with the velocity contour patterns and the bed shear stress found on Figure 9 and Figure 10. Peak zones of shear stress and velocity contour are ultimately the causes of high scour in the streambed. A similar trend has been observed in natural rivers (Lim, 1993; Lim and Cheng, 1998). At the bend, as it expected, there are erosion patterns. Secondary currents are driven by the combined pressure force of the transverse superelevation and the centrifugal force; their magnitudes are about one order less that that of the streamwise flow (Nezu and Nakagawa, 1993). Therefore, they contribute to the moving of the sediments and consequently to streambed degradation. Towards the downstream end of the channel it is expected that the bed may be lowered as the flow picks up more energy upon leaving the hole at cross section (1). However, deposition patterns in the streambed occur in zones where the velocity magnitudes and bed shear stress are low. For example, when the channel width increases, it is expected the flow velocity, flow depth, and shear stress decrease, which ultimately leads to deposition of the transported material.

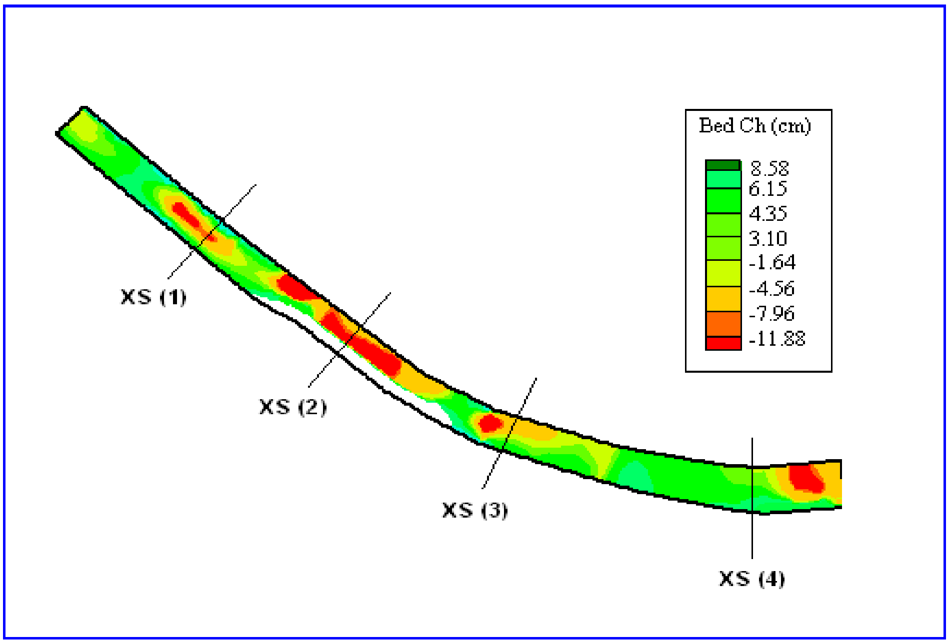

Figure 11. Modeling Results for Changes in the Bed Elevation for Scenario (1)

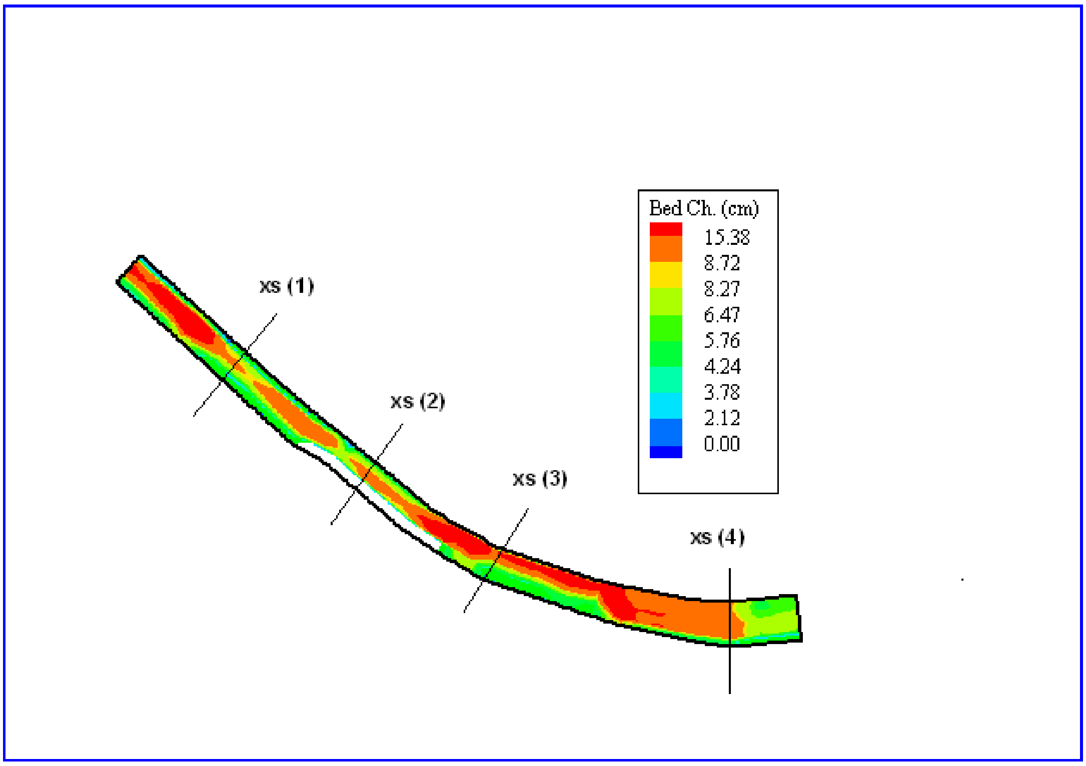

Figure 12: Modeling Results for Changes in the Bed Elevation for Scenario (2)

Table 6: EnSEDZL Model Predictions for the Bedload Transported Material in the Stream for the Two Modeling Scenarios and a Comparison with the Measured Data.

Method	Size ranges (mm)				Total bedload (Tons/day)
	<0.85mm	0.85-6.3 mm	6.3-9.5 mm	>9.5mm	
EnSEDZL prediction Scenario 1 (2-yr)	1.3244	4.1824	0.1305	0.1326	5.7699
EnSEDZL prediction Scenario 2 (10-yr)	9.7626	5.2831	0.7905	1.3176	17.1538
Measured Tons/day	2.22	3.76	0.26	0.81	7.05

Conclusions

To this end, an integrated watershed sedimentation tool has been developed and applied to simulate macro to micro-level sediment transport and geomorphic processes in a river basin. An upland erosion model has been coupled with a coupled 2-D instream averaged-depth hydrodynamic and multifractional sediment transport model. Multiple spatial and temporal scale watershed processes were investigated. The GeoWEPP model, a soil erosion model, was selected and employed in this study since it can handle the spatial and temporal scale variability in watershed processes. The model was run using different subwatershed sizes over a long and short period of times and both long term averages and frequency distribution analyses for the sediment yield rates were obtained.

To accurately address the scale and coupling issues, a thorough investigation for the particle transit time was performed at three levels following the particle travel paths within a watershed. The state of the art concepts on particulate travel time were used, including the hypsometric curve approach and the particle virtual velocity approach. It was demonstrated that a fine sediment particle moves from the uplands to the mouth of the watershed within a relatively short period of time (few days). Therefore, the assumption made was that there is approximately no lag time between the sediment generated at the uplands and that which transported in the stream. It was not surprising that the particle virtual velocity approach showed more reasonable ranges for the travel time (i.e., on the order of days) when compared with the hypsometric curve approach, which showed minimum travel time ranges (on the order of seconds). Nevertheless, the particle virtual velocity approach was developed for instream flows when coarse sediment particles move on a rough surface. This approach employed herein based on an analogy with the upland soil erosion process, where a fine particle moves on vegetated surface. Vegetation in upland soil erosion process is protruding the flow in a similar way that the rough elements do in the stream.

The integrated framework has been applied to the Main Fork Red River watershed. Results computed by the soil erosion model show that for a 2-yr rainfall storm event the sediment yields compared closely with the data measured for the suspended loads in the river. However, long-term averages indicate that the model overestimates the observed sediment yields. For the instream model, the computed results indicate the model is very sensitive to the sediment supply. The model was able to predict the right channel bathymetry only when the correct values for the sediment yield are considered. The modeling scenario using the 10-yr event for sediment load was illustrated the streambed adjustments sensitivity to the input of upland sediment load.

Comparison of the model calculations against another 2-D and 1-D models indicate that single class 2-D sediment transport models which was developed mainly for uniform sediments are inappropriate to simulate nonunifrom sediment transport with an effective diameter. These models do not account for the heterogeneity that exists in the bed and consequently lead to poor predictions. However, a 1-D model is still a potentially useful tool in geomorphological studies if the right equations are incorporated.

References

Ackers, P. and W.R. White. 1973 Sediment Transport: "A New Approach and Analysis." *Journal of the Hydraulics Division, American Society of Civil Engineers*. Vol. 99

Al Espinosa, F. Jr., Rhodes, J. J., and McCullough, D.A., 1997. "The Failure of Existing Plans to Protect Salmon Habitat in the Clearwater National Forest in Idaho." *Journal of Environmental Management*. 49:205-230.

Andrews, E.,1984. 'Bed-material entrainment and hydraulic geometry of gravel bed rivers in Colorado." *Geological Society of America Bulletin* 95: 371-378.

Ascough II, J.C., Baffaut, C., Nearing, M.A., Liu, B.Y., 1997. 'The WEPP watershed model: I. Hydrology and erosion." *Trans. ASAE* 40(4): 921–933.

Ashida, K. and Michiue, M., 1971. "An investigation of riverbed degradation downstream of a dam." *Proc. 14th Congress of the IAHR.*

Baffaut, C., Nearing, M.A., and Nicks, A.D., 1996. "Impact of CLIGEN parameters on WEPP-predicted average annual soil loss." *Trans. ASCE,* 39(2): 447-457

Bagnold, R. A. 1977. "Bed load transport by natural rivers." *Water. Resour. Res.*, pp.303-312

Bernard, J., and Thomas, I., 2000. “Sediment Damages and Recent Trends in The United States.” *International Journal of Sediment Research*,15 (2):135-148.

Bonniwell, E. C., Matisoff, G., and Whiting, P.J., 1999. “Determining the time and distance of particle transit in a mountain stream using fallout radionuclides.” *Geomorphology*, 27, 75-92.

Borah, D.K., Alonso,C.V., and Prasad, S.N., 1982. “Routing graded sediments in streams: Formulations.” *J. of Hydraulic Engineering, ASCE,* 108:1486-1503

Bunte, K, and MacDonald, L.H., 1999. “Scale considerations and the detectability of sedimentary cumulative watershed effects.” *Tech. Bull. 776. Research Triangle Park,* NC: National Council for Air and Stream improvement. 327 p.

Burban, P.Y., Xu, Y., McNeil, J., and Lick, W., 1990. “Settling speeds of flocs in fresh and seawaters.” *J. Geophysics Res.* 95(C10)L 18213-18220

Cardenas, M., Gailani, J., Zeigler, C.K., and Lick, W., 1995. “Sediment transport in the lower Saginaw River.” *Mar. Freshwater Res.*, 46, 337-347

Chang, H., 1992. *Fluvial processes in river engineering*. John Wiley and Sons Inc.

Christofferson, J.B., and Jonsson, I.G., 1985. “Bed friction and deposition in a combined current and wave motion.’ *Ocean Engineering*, 12:387-423

Chen, Y.H., 1988. “Development of a quasi-non equilibrium reservoir sedimentation model: RESSED.” *Proc. Second Seminar on Stream Sedimentation Models, Sedimentation Subcommittee*, Interagency Advisory Committee on Water Data, Oct.

Cheng, N.S., 1997. “Simplified settling velocity formula for sediment particle.” *ASCE J. of Hydraulic Engineering,* 123(2): 149-152

Dietrich, W.E., 1982. “Settling velocity of natural particles.” *Water Resources Research.* 18(6): 1615-1626

Diplas, P., 1987. “Bedload transport in gravel-bed streams.” *J. Hydraul. Engrg., ASCE*, 113(3), pp. 277-292

Elliot, W. J., and D. E. Hall. 1997. “Water Erosion Prediction Project (WEPP) forest applications.” *General Technical Report INT-GTR-365.* Ogden, UT:

U.S. Department of Agriculture, Forest Service, Rocky Mountain Research Station.

Elliot , W.J., Scheele, D.L., and Hall, D.E., 2000. “The Forest Service WEPP interface.” *Paper No. 00502*1. St. Joseph, MI, *ASCE*. 9p.

Elliot, W.J.; Robichaud, P.R.; Pannkuk, C.D. 2001. “A Probabilistic Approach To Modeling Erosion for Spatially-Varied Conditions*.” Proceedings of the Seventh Federal Interagency Sedimentation Conference*, March 25 to 29, 2001, Reno, Nevada. Volume 2, Section VI, "Data Quality Assurance." p. VI-33 -- VI-40.

Elliot, W. J., and Robichaud, P.R., 2001. “Comparing erosion risks from forest operations to wildfire.” *The International Mountain Logging and 11th Pacific Northwest Skyline Symposium.*

Elliot, W., and Miller, S., 2002. “Estimating erosion impacts from implementing the national fire plan.” *ASAE annual international meeting/CIGR XVth world congress*. Chicago, IL, July 28- July 31.

Engelund, F., and E. Hansen. 1972. “A monograph on sediment transport in alluvial streams.” *Tekn ,isk Vorlag, Copenhagen.*

Favis-Mortlock, 1998. “Validation of field scale soil erosion models using common datasets.” In: J. Boardman and D. Favis-Mortlock, Editors, *Modeling Soil Erosion by Water NATO ASI Ser.*, Ser. I vol. 55, Springer-Verlag, Berlin, Germany , 89–127.

Finker, S.C., Nearing, M.A., Foster, G.R., and Gilley, J.E., 1989. “A simplified equation for modeling sediment transport capacity.” *Trans. ASAE*, 32(5): 1545-1550.

Flanagan, D.C., and Nearing, M.A., 1995. “USDA-Water erosion prediction project hillslope and watershed model documentation.” *NSERL Report,* vol. 10. USDA-ARS National Soil Erosion Research Laboratory, West Lafayette, IN.

Flanagan, D.C., Fu, H., Frankenberger, J.R., Livingston, S.J., Meyer, C.R., 1998. “A Windows interface for the WEPP erosion model.” *Annual International Meeting of the American Society of Agricultural Engineers*. Orlando, FL, 14 pp.

Foster, G.R., Young, R.A, and Neibling, W.H, 1985. “Sediment composition for nonpoint source pollution analyses.” *Trans. ASAE* 28:133-139

Foster, G.R., 1982. “Modeling the erosion process.” Chapter 8 in: C.T. Haan (Ed.), *Hydrological modeling of small watersheds. ASAE Monograph*, No. 5, St. Joseph, MI. pp. 297-360.

Gailani, J., Ziegler, C.K., and Endicott, D., 1996. “Development and calibration of a fine-grained sediment transport model for the Buffalo River.” *Journal of Great Lakes Research,* 22:765-778.

Gallaher, D., 1999. “The three leading killers of GIS.” Proc. *for URISA, Annual meeting*, Chicago, IL, CD-ROM Publications.

Gessler, J., 1967. “The beginning of bedload movement of mixtures investigated as natural armoring in channels.” *W.M. Keck Laboratory of Hydraulics and Water Resources, California* Institute of Technology, Translation T-5

Ghidey, F., Alberts, E.E., 1996. “Comparison of measured and WEPP predicted runoff and soil loss for Midwest claypan soil.” *Trans. ASAE*, 39(4): 1395-1402

Gloss, D., 1995. “Evaluation of the NEZSED sediment yield model using data from forested watershed in north-central Idaho.” *M.Sc. Thesis.* University of Idaho, USA.

Gove, N., Edwards, R., and Conquest, L., 2001. “Effects of Scale on Land Use and Water Quality Relationships: A Longitudinal Basin-Wide Perspective.” *Journal of The American Water Resources Association*. 37(6): 1721-1734.

Guo, Q., and Jin, Y.C., 1999. “Modeling sediment transport using depth-averaged and moment equation.” *Journal of Hydraulic Engineering*, 125(12): 1262-1269

Han, Q., and He, M., 1987. “Mathematical model of reservoir sedimentation.” *Journal of Sediment Research,* 3, 14-29

Harmon, J., N., Gerhardt, and D. Green, 1992. *NEZSED User’s Guide*. 3rd Edition. Unpublished document, Nez Perce National Forest, Grangeville, ID.

Hatfield, T., and Bruce, J., 2000. “Predicting Salmonid Habitat-Flow Relationships for Streams From Western North America.” *Journal of Fisheries Management*. 20: 1005-1015.

Holley, F.M., and Usseglio-Polatera, J.M., 1984. “Dispersion simulation in two dimensional tidal flow.” *Journal of Hydraulic Engineering, ASCE*, 110(7)

Interagency Advisory Committee on Water Data (IACWD), *Guidelines for Determining Flood Flow Frequency, Bulletin #17B* of the Hydrology Subcommittee, Revised September 1981, Editorial Corrections March 1982.

Jia, Y., and Wang, S. 1999. “Numerical model for channel flow and morphological change studies.” *Journal of Hydraulic Engineering,* ASCE, 125(9): 924-933

Karim, M.F., and Holly, F.M., 1986. “Armoring and sorting simulation in alluvial rivers.” *J. of Hyd. Engineering, ASCE*, 112(8): 705-715

Kassem, A., and Chaudhry, M., 2002. “Numerical modeling of bed evolution in channel beds.” *J. of Hyd. Engineering*, 128(5): 507-513

King, I.P. and W.R. Norton, 1978. “Recent Application of RMA's Finite Element Models for Two Dimensional Hydrodynamics and Water Quality.” *Finite Elements in Water Resources*, Pentech Press, London.

Kleinhans, M., 2002. “Sorting out sand and gravel, sediment transport and deposition in sand-gravel Bed Rivers.” *Ph.D. Thesis*. University of Netherlands, the Netherlands.

Kleinhans, M.G., Leo, C., and Rijin,v., 2002. “Stochastic prediction of sediment transport in sand-gravel bed rivers.” *Journal of Hydraulic Engineering*, 128(4): 412-425.

Knapp, D. 2002. “Applications of Particle Velocity to Bedload Motion.” *M.Sc. Thesis.* Washington State University, Pullman, USA.